Are Sea State Measurements Required for Fatigue Load Monitoring of Offshore Wind Turbines?

U Smolka, D Kaufer and P W Cheng
Stuttgart Wind Energy Research (SWE), Universität Stuttgart, Germany
E-mail: Ursula.Smolka/Daniel.Kaufer/PoWen.Cheng@ifb.uni-stuttgart.de

Abstract. Neural network algorithms have shown the capability to infer the actual wind turbine loading from standard signals commonly used for operational control purposes. Fatigue load monitoring done with this readily available data, can offer a robust and cost effective alternative to conventional maintenance-intensive mechanical stress measurement devices. The concept needs to be adopted to offshore wind turbines, where the exposure to the harsh environment with rather difficult accessibility makes the use particularly attractive. At such a site the impact of hydro-dynamically dominated loads might result in poor fatigue estimates, which is due to the lack of information on the surrounding sea state. In order to avoid the need of measuring-buoys, this work studies the employment of additional accelerometers mounted directly at the structure. Various potential placements and three sub-structure types are considered to account for the characteristic structural response caused by wave induced loading. The feasibility is demonstrated on generic data, gained from simulations. Recommended practices are deduced and applied to data from the AREVA M5000 turbine at "alpha ventus".

1. Introduction

Conventional fatigue load monitoring is done with mechanical stress measurements. For reasons of costs and reliability of the measuring devices it is applied on prototypes for a limited period of time only. Therefore knowledge of long-term site specific accumulated loading of wind turbines is difficult to obtain. A fatigue load monitoring system based on standard signals, such as electrical power, generator speed and pitch angle conventionally measured for operational control purposes can be used to infer the actual loading of the wind turbine with the use of artificial neural networks [1]. The accuracy of the load estimation has been evaluated for field data of offshore wind turbines with monopile [2] and tripod type sub-structures [3]. In both cases poor results were obtained where wave induced loads play a dominant role.

Relying on standard signals only, the estimation of fatigue loads acting on the structure above the sea surface works well in normal operating condition, as the sea state is highly correlated with the wind speed measured at the hub height. However, under the same condition the estimation of structural loading under the water surface does not produce acceptable results, due to the influence of currents. Furthermore poor results are obtained for all structural fatigue loads occurring under parked or idling operational conditions. But due to the absence of aero-dynamical damping in idling condition the wave impact on the structure is passed to the tower top. If acceleration signals are available, the information on hydrodynamic loading can be extracted by the neural network to some extent. Without sea state measurements a comprehensive overall load monitoring system that relies on standard data only is not feasible.

There are fatigue loads of interest that can only be estimated when the sea state measurements are available to provide a direct correlate to the structural response of the loaded wind turbine.

This work focuses on improving fatigue load monitoring for loading situations where non standard sea state measurements are required in theory for an accurate estimation. It is suggested to extend the number of standard signals with additional accelerometer measurements, originating from devices mounted directly at the support structure. Therefore a method to derive an optimal accelerometer configuration is introduced. Eventually, it is the goal to identify a substitute for expensive oceanographic sensors while providing similar or even better load monitoring quality.

In the scope of this paper, a short overview on the design of the study and fatigue load monitoring based on standard signals is given first. Then the verification of the load monitoring with added accelerometers is done in Section 3 by conducting IEC compliant simulations under coupled wind and wave dynamics [4] for different support structure types. The simulation results constitute a generic data base as it is not taken from real measurements and used to systematically evaluate the estimation accuracy of wave induced fatigue loading, by varying the information content provided to the neural network. The achievable accuracy and optimal placement of the accelerometers at the support structure of the wind turbine is discussed in Section 4. Based on the established method and recommendations, fatigue load monitoring with added accelerometers instead of sea state measurements is demonstrated in Section 5 using one year of measurement data from the test site "alpha ventus" for the AREVA M5000 tripod type support structure.

2. Wind Turbine Parameters and Load Cases

The characteristic interaction of support structures with the surrounding sea state has lead to a variety of fixed-bottom concepts realized in the offshore industry. Their suitability to specific offshore sites result from the assumed design fatigue and extreme loads which are driven by a combination of aero- and hydrodynamical environmental parameters. In order to assess the potential of the suggested monitoring of hydrodynamic loads on the basis of accelerometer data, key aspects such as sub-structure type, simulation tool, simulation set-up and load cases have been considered in the present analysis. While the simulation time series gained serve as a generic dataset for the design and general evaluation of the load monitoring system, the AREVA M5000 turbine sited at "alpha ventus" is the source of field data used to apply the concept.

2.1. Offshore Turbine Model Description

Three common sub-structure types were chosen that show a distinct structural response to hydrodynamic loading [5]. The monopile type sub-structure is most frequently applied at shallow water sites up to 25 m water depth. As a matter of stiffness, large diameters are required that attract relatively high hydrodynamic loads. For deeper sites a collection of slender members that let the water masses pass relatively unobstructed is favoured as sub-structure. Tripods and jackets belong to this class. Due to a usually wide base their resistance against overturning is affected by the directionality of wind and wave loads.

The generic offshore wind turbine models used are publicly available and rely on the achievements of the UpWind project [6] to design a jacket for 50 m of water depth and the IEA Wind Annex 23 Subtask 2 - Offshore Code Comparison Collaboration (OC3) [7] to design a monopile and tripod for water depths of 20 m and 45 m respectively. All sub-structure types designed were adopted to carry the generic wind turbine developed by NREL [8]. The turbine is a representative of the 5 MW class, designed by averaging and extrapolating basic parameters of wind turbines on the market. This wind turbine is a conventional three-bladed, upwind, variable speed, variable pitch to feather controlled turbine. The specifications consisted of

detailed aerodynamic properties, structural data for blades, tower, nacelle and drive-train. The original controller of this turbine has been changed by an in-house optimized controller.

The AREVA M5000, with properties and parameters that are comparable to the NREL turbine, is supported by a tripod sub-structure in water depth around 28 m. An overview of the four turbines' specification is given in Table 1.

Table 1. Specifications of the generic models and the AREVA M5000 turbine used in the study. Generic data is generated from FLEX5 - Poseidon fully integrated simulations, while field data was recorded at the test field "alpha ventus" in the North Sea.

	generic model			"alpha-ventus"
	OC3 monopile	UpWind jacket	OC3 tripod	AREVA M5000
rated power		5 MW		5 MW
rated wind speed		11.4 $\frac{\mathrm{m}}{\mathrm{s}}$		12.5 $\frac{\mathrm{m}}{\mathrm{s}}$
rotor-nacelle mass		350 t		309 t
tower mass		348 t		348 t
1st tower eigenfrequency	0.278 Hz	0.261 Hz	0.282 Hz	– Hz
sub-structure mass	285 t	676 t	826 t	– t
water depth	20 m	50 m	45 m	28 m

2.2. Simulation Assumptions and Load cases

Acceleration measurements play the major role in the detection and estimation of hydrodynamic loads within this work. Therefore, a fully integrated time domain analysis is required to assure a proper computation of the interaction between sea-state and structural response. The fatigue load simulations are conducted with Flex5-Poseidon [4] to produce meaningful time series. As a function of wind speed, the operational behaviour and thus the loading characteristic of wind turbines in power production and idling mode differs significantly. A total of nine independent wind seeds for each $1\frac{m}{s}$ bin in the range from from $4\frac{m}{s}$ to $25\frac{m}{s}$ are used in IEC compliant fatigue load simulations for both power production and idling operation mode of the three generic turbines. Transient events were not considered in the simulation nor within the measurements. All environmental conditions are extracted from the design basis of "alpha ventus" for one inflow sector and binned wind speed with a unique sea state assigned to[9]. To spread the loading a slight misalignment of $\pm 4°$ between turbulent wind and the sea state are overlaid for six out of nine total seed numbers. The inflow sector is not changed at all, such that the directionality in wind and wave loading is neglected in the analysis. In total, 198 ten minute time series with a sampling rate of 50 Hz are simulated for each turbine, equal to 66 hours of operation. The amount of data and the sampling rate meets the specific needs in the training procedure of the neural network for the anticipated load monitoring discussed in Section 4.

3. Neural Network Configuration for Fatigue Load Estimation

The discussed load monitoring system profits from the capability of artificial neural networks (ANN) to establish complex non-linear mapping function. Their ability to classify, to organize and to learn from sample data is established during an iterative training process where a number of corresponding input-output data pairs are presented to the network. A random configuration of the networks weights which describe an addition and division calculation rule of the input values, is the starting point. Then the involved algorithm brings the network's output (estimate) closer to the desired output (target) by adapting the network configuration appropriately. As

the network is made to learn the dynamics of the wind turbine based on presented input-output data pairs, no modelling equations and a-priori knowledge as needed for physics based models are required. The learning algorithm processes generic and real turbine data equally. The resulting network is specific to the (generic) turbine and uses the once identified mapping function between target and input, to compute an estimate when new input data is available. A more elaborate description on the set up of feed-forward single layer neural networks for fatigue load monitoring of offshore wind turbines can be found in [3] while a more general introduction is given in [10].

In the present context, a set of ten minute based aggregated values of four standard signals serve as basic input to the neural network. The fifth signal is kept variable to assess the quality of the load estimation procedure depending on non-standard signals. Besides the significant wave height, four individual lateral and longitudinal accelerometer signals are used, originating from distributed locations at heights from the tower top till the sub-structure. The aggregation of high resolution signals can be done by considering various statistical quantities and aggregates.

The list below gives an overview of the signals and corresponding statistics, all used as a set of input variables for one feed-forward neural network:

(i) **yaw misalignment:** mean, std. dev.
(ii) **generator speed:** min., mean, max., std. dev. and equivalent range value
(iii) **electrical power:** min., mean, max., std. dev. and equivalent range value
(iv) **pitch angle:** min., mean, max., std. dev. and equivalent range value
(v) **swapped (non-)standard signal:** either significant wave height or std. dev. and equivalent range of acceleration.

To allow for a mapping between fatigue loads and standard signals, it is sufficient to derive ten minute aggregates that reduce the complexity of the dynamic characteristics of disturbances and loads [1]. The load estimation procedure will work satisfactory with mean, minima (min.), maxima (max.) and standard deviation (std. dev.) values applied on the signals on the input side of the neural network. As a new feature in contrast to [1],[2] and[3], rain-flow counted equivalent signal range values of the high resolution inputs were added as well. The computation is done for the same Wöhler constant and reference cycle number as for the fatigue load cycle computation. By transferring the strong non-linearity to the inputs that is present in the fatigue load cycle computation, a higher estimation accuracy could be achieved. On the output side, equivalent load ranges are commonly used to describe fatigue loads. They allow to characterize the fatigue impact of a distinct loading time series with just two parameters. For the evaluation of the suggested method in total four hydro-dynamically influenced load signals have been selected: longitudinal tower base bending moment and overturning moment for all three sub-structure types, local axial strain for one slender member oriented vertically at the jacket sub-structure base and finally the local strain at two of the tripod braces with horizontal and diagonal orientation with respect to the seabed. Each of these load quantities required two neural network trainings, one for the power production and one for the idling condition. Finally, all settings and configurations that influence the quality of the estimation are maintained during the whole study, both for generic and for field measurement data. The trainings and evaluation of the neural network were conducted using $MATLAB^{®}$ and the freely available $NNSYSID$ Toolbox of the Technical University of Denmark [11].

4. Evaluating the Use of Additional Accelerometer Data

4.1. Achievable Estimation Accuracy

The configurations defined in Section 3 consist of a set of standard signals, one non-standard signal and the load quantity to be estimated. For each of these configurations and data from

two operational conditions - power production and idling - a neural network has been trained with data from six seeds out of nine total per wind bin. The remaining time series from the three seeds per bin are used to test the trained neural network for its capability the estimate fatigue loads from the data it has not seen before. The accuracy is given as the root mean square (RMS) estimation error of the test data as listed in table 2 for the best configurations found. The smaller the value, the better the information on the overall fatigue loading can be

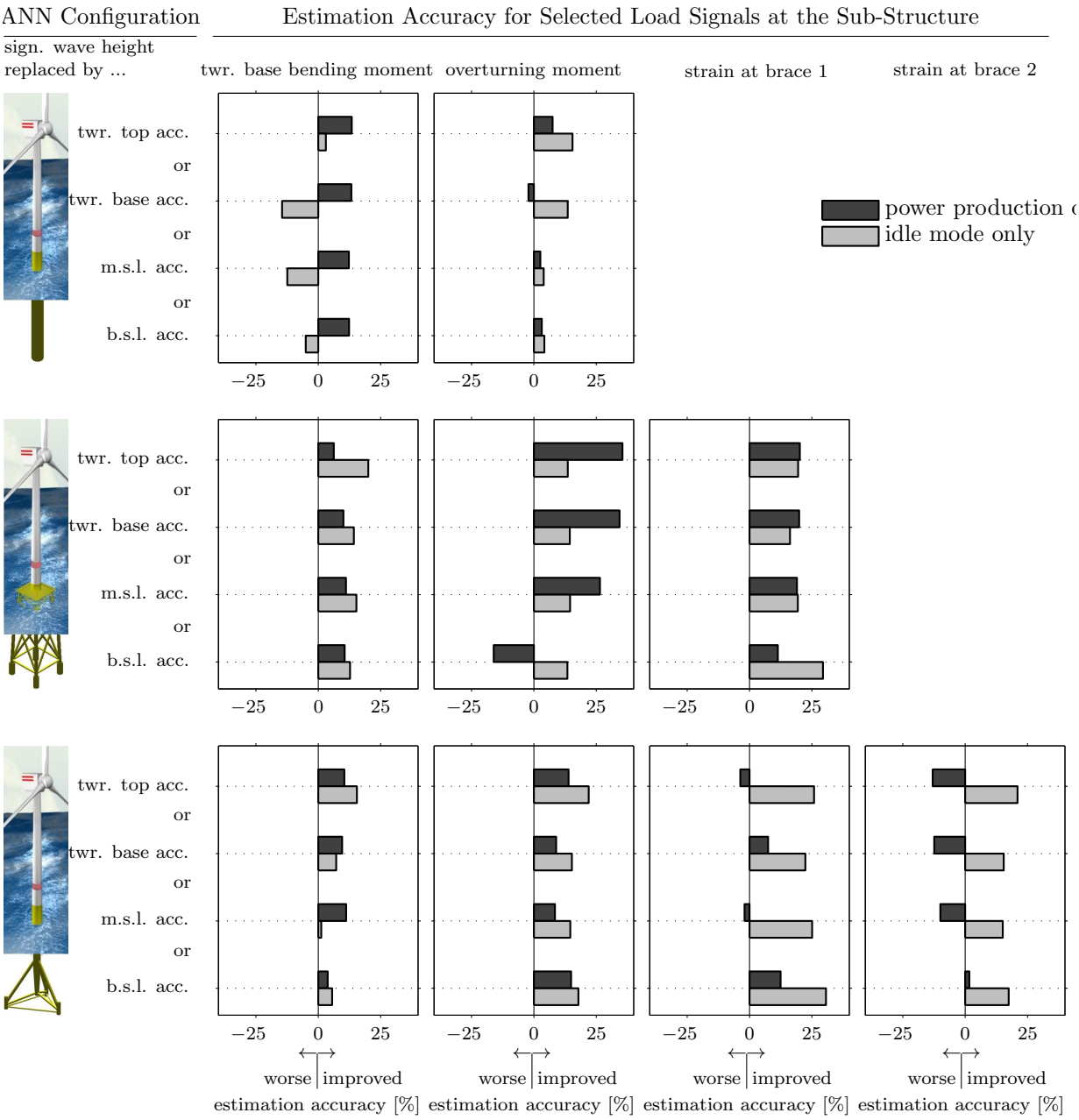

Figure 1. Relative estimation accuracy when replacing the significant (sign.) wave height signal by acceleration signals either originating from the tower (twr.) top or the tower bottom or the support structure at mean sea level height (m.s.l) or from below the sea level (b.s.l).

inferred by the neural networks' learning algorithm from the selected inputs. The reasons for changes in accuracy within the various configuration are plenty. For example the presence or absence of aero dynamical damping, the dominance of hydrodynamical loads, the interaction of the sub-structure with passing water masses or the added information on aerodynamical loading by adding new inputs. Within the scope of this work this is not elaborated on. Instead Figure 1 contains a useful summary on the substitutability of sea state measurements.

Figure 1 gives an overview of the achievable accuracy using different accelerometer signals and relates the results to the configuration where the significant wave height is assumed available. As an example, the longitudinal tower base bending moment of the analysed wind turbine with monopile sub-structure can be equally well estimated using tower top accelerometer measurements rather than the significant wave height signal. A closer look reveals that the accuracy has even improved by 13% for power production modes and by 3% for idling. Moving on to the overturning moment in the same row of the figure, it is striking that all chosen accelerometer signals do outperform the reference configuration by $(4\% - 15\%)$ in idling mode, and under performs just once in power production mode by around 2%. Reviewing all other wind turbines with their load signals analysed, it is apparent that one can always find an accelerometer signal that can replace sea state measurements, independently from the sub-structure type and independently from the load quantity to be estimated. In some cases it might be even attractive and necessary to install two accelerometer devices to get best results: whereas the monopile and jacket type sub-structure loads show an improved estimation accuracy with the use of tower top accelerometer signals only, the tripod brace 1 and brace 2 loads require an additional accelerometer device mounted on the structure below the sea level.

4.2. Practical Recommendations

It has been shown that the use of accelerometers facilitates the replacement of sea state measurements and even has the potential to lead to better fatigue load estimation results. To find the best configuration for a specific load estimation task, several aspects like the accessibility for maintenance and installation routines, robustness of the device and investment are to be included. As an example it might be tolerable to loose accuracy in estimating the local loads on the tripod braces by saving costs for the operation of a measuring buoy or an additional acceleration sensor with poor accessibility. Considering the operational time that the turbine will be in power production mode, a higher estimation accuracy in that mode is favourable.

Based on the findings above for each sub-structure type a new neural network has been trained to cope with data from both idling and power production mode, using accelerometer signals that lead to the highest achievable accuracy. Figure 2 shows the RMS error of the longitudinal tower base bending moment for the idling modes trained separately and combined, binned over the mean wind speed. It is apparent that all three sub-structure types exhibit a similar behaviour, with a peak around the rated wind speed in power production mode and an approximately linear rise in the RMS error with rising wind speed in idling mode. Therefore it can be stated that the transition region between partial and full load constitutes a severe challenge for the estimation procedure that is based on ten minute statistics only. Equally high errors are obtained when the turbines are idling at wind speeds higher than 20 $\frac{m}{s}$. The last graph demonstrates the capability of the neural network to process the available inputs in an optimal way, where the RMS error is balanced between the occurrence of both operation modes. Table 2 summarizes the results for the best accelerometer signal configuration along with the significant wave height configuration by displaying the absolute mean estimation error with its standard deviation.

5. Application to Field Data

The database employed in this study consists of one year of "alpha-ventus" test-field data (2010/05 - 2011/04) of the AREVA M5000 with turbine properties listed in Table 1. Figure 3

Table 2. Mean estimation error [%] and standard deviation for the studied generic models. Only significant wave height and best accelerometer configuration is listed.

	twr. base bending moment	overturning moment	strain at brace 1	strain at brace 2
monopile				
sign. wave height	0.49 ± 8.33	0.17 ± 7.13		
twr. top	1.36 ± 7.71	0.56 ± 5.04		
jacket				
sign. wave height	0.36 ± 9.96	1.34 ± 7.22	0.73 ± 8.32	
twr. top	0.66 ± 8.97	0.15 ± 4.34	0.28 ± 5.40	
tripod				
sign. wave height	1.68 ± 10.62	0.73 ± 10.69	0.54 ± 10.67	1.43 ± 7.05
twr. top & b.s.l. acc.	0.93 ± 4.66	0.23 ± 4.81	0.92 ± 6.00	0.36 ± 5.03

a) shows a photo-montage of the turbine and a draft of the tripod (not to scale). Compared to the generic tripod type sub-structure, the horizontal braces in the lower part, connecting the pile sleeves, are missing. But due to the overall geometric similarity, the best accelerometer configuration derived in the simulation study, is chosen. The data portion used includes standard signals listed in Section 3 and additional non-standard acceleration data from the tower top and below the sea level in lateral and longitudinal direction. The position of these sensors are marked with a blue diamond in Figure 3 a).

To allow for a comparison with the reference study case, the estimation routine that includes the significant wave height measurements is considered as well. Except for the significant wave height which is recorded by a buoy at the research platform FINO 1 in a distance of

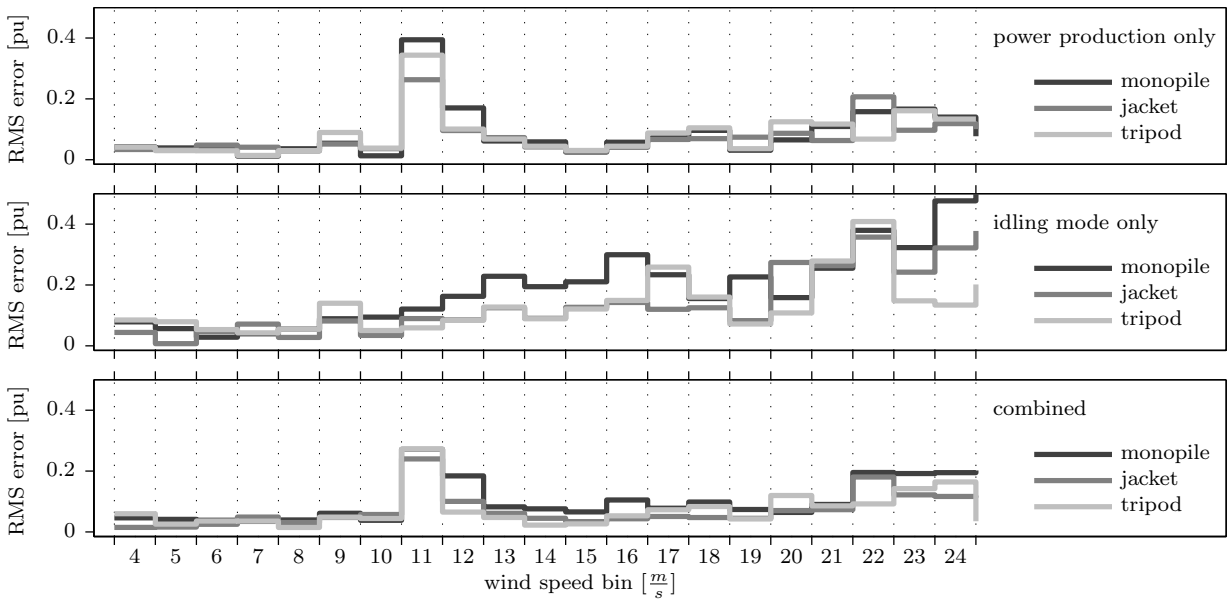

Figure 2. Estimation accuracy of simulated longitudinal tower base bending moments for two operation modes and their combination, using accelerometer signals.

approximately 700 m of the test turbine, all measurements are sampled at 50 Hz and aggregated to ten minute statistics and equivalent ranges. According to the damage accumulation hypothesis the equivalent load range is computed for three out of the four discussed fatigue loads. The grey striped pattern at the lower leg brace 1, upper leg brace 2 and main column of the tripod in Figure 3 a) mark the sensor locations used for longitudinal tower bottom bending moment and local strain computations. The overturning moment is not available as evaluated quantity, due to sensor failure.

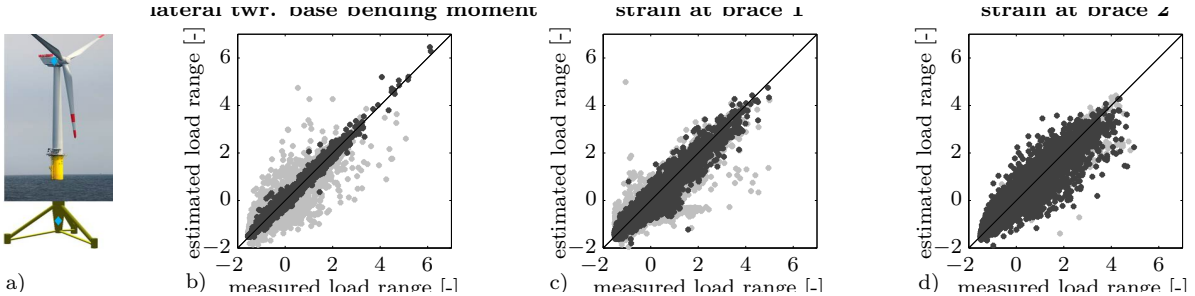

Figure 3. Regression plot of estimated versus measured fatigue loads with two different neural network configurations: light grey using only significant wave height and dark grey using best accelerometer. The values are normalised using mean and standard deviation values from the training data set.

During the twelve month of operation the turbine experienced mean wind speeds of up to 28 $\frac{\mathrm{m}}{\mathrm{s}}$ with mean turbulence intensities ranging from 5 % to 18 % and wave heights of up to 6 m during idling, parked and power production modes in wake and free inflow conditions. Including a total of 29823 ten minute data samples used in the validation of the concept, demands a higher computational effort for the training process than in the case of the generic dataset used in the preliminary studies. But the variety of environmental and operational conditions present in the dataset is desirable. The regression plots displayed in Figure 3 b) to d), give an impression about the capability of the neural network to cope with the noise under real conditions. For the longitudinal tower bending moment, the light grey scatter plot in Figure 3 b), which show the results that are obtained with the sea state measurements configuration, is wider than the dark grey scatter, that represents the results of the best accelerometer configuration. The significant improvement in estimation accuracy, with absolute values given in Table 3, are expected due to the aerodynamic loading information that is present in the tower top acceleration measurement. Moving on to the loads below the water surface, where wave loading is expected to have a stronger impact, the benefit of using accelerometer data is apparent for the estimation of the local strain range at the lower leg (brace 1). However, the estimation accuracy for the local strain range at the upper leg (brace 2) is worse compared to the use of the significant wave height information. But as argued before, even in this case the use of the accelerometers should be considered as valuable replacement for sea state measurements. After all, better than nothing: without acceleration and sea state measurements the estimation error would reach a much higher value at 18.01 ± 60.31. Therefore, it holds for all load quantities, that the use of accelerometer data is of advantage, as it makes sea state measurements superfluous for the suggested fatigue load estimation.

6. Conclusions

From three publicly available offshore wind turbine models a generic dataset is derived by conducting IEC conform fatigue load simulations. These data samples are then used to train and

Table 3. Mean and standard deviation of the fatigue load estimation error [%] for two neural network input configurations with data from one year of operation of the AREVA M5000.

	twr. base bending moment	strain at brace 1	strain at brace 2
sign. wave height	8.46 ± 38.90	5.53 ± 22.66	2.13 ± 15.73
twr. top & b.s.l. acc.	0.51 ± 7.73	2.98 ± 16.80	5.77 ± 26.89

evaluate neural networks for fatigue loads estimation. A method has been presented that allows to easily determine weather, with a given standard data configuration, sea-state measurements are dispensable by additional accelerometer data. For three common sub-structure types, monopile, jacket and tripod, it has been shown that with accelerometers even a higher estimation accuracy might be achievable. Furthermore the results obtained from simulation studies, suggest that the characteristic interaction of waves with the sub-structures demands a specialized load monitoring system design with accelerometer placements that depend on the load quantities to be estimated. The optimal placement might be chosen advantageous in terms of accessibility for maintenance. Finally, the recommendations are applied to a standard data based load monitoring system for field data from the AREVA M5000 at "alpha ventus" which demonstrates the feasibility of a load monitoring system without the need of sea state measurements.

Acknowledgements
This research is funded by the German Federal Ministry for the Environment, Nature Conservation and Nuclear Safety (BMU) in the framework of the German joint research project "RAVE - OWEA. Verification of offshore wind turbines" (FKZ 0327696A-D). The authors further acknowledge the cooperation with the AREVA Wind GmbH, Bremerhaven, and the possibility to validate the presented approach on the basis of measurement data.

References

[1] Cosack N 2011 *Fatigue load monitoring with standard wind turbine signals* Ph.D. thesis Faculty of Aerospace Engineering and Geodesy of the Universität of Stuttgart Germany

[2] Obdam T, Rademakers L and Braam H 2010 *Wind Engineering* **34** 109–122

[3] Smolka U, Quappen J, Siegmeier B, Kühn M and Cheng P W 2011 Fatigue Load Monitoring for a Tripod Support Structure Based on Standard Wind Turbine Signals *Proceedings of the European Wind Energy Association, OFFSHORE* (Amsterdam, The Netherlands)

[4] Kaufer D, Cosack N, Böker C, Seidel M and Kühn M 2009 Integrated Analysis of the Dynamics of Offshore Wind Turbines with Arbitrary Support Structures *Proceedings of the European Wind Energy Association, EWEC* (Marseille, France)

[5] de Vries W, Vemula N K, Passon P, Fischer T, Kaufer D, Matha D, Schmidt B and Vorpahl F 2011 Final report EU-UpWind-Project Task 4.2 - support structure concepts for deep water sites Final report Delft University of Technology Delft, The Neatherlands

[6] Fischer T and de Vries W 2011 Final report EU-UpWind-Project Task 4.1 - offshore foundations and support structures Tech. rep. Endowed Chair of Wind Energy, Universität Stuttgart Germany

[7] Jonkman J and Musial W 2010 Offshore Code Comparison Collaboration (OC3) for IEA Task 23 Offshore Wind Technology and Deployment Technical Report NREL/TP-5000-48191 National Renewable Energy Laboratory Boulder, USA

[8] Jonkman J, Butterfield S, Musial W and Scott G 2009 Definition of a 5-MW reference wind turbine for offshore system development Technical Report NREL/TP-500-38060 National Renewable Energy Laboratory Boulder, USA

[9] Dörfeldt S and Bicker S 2007 Design Basis, Standort "Borkum West" - Projekt "alpha ventus" Tech. Rep. DOTI.P02.G01.DB.001 - RO Offshore Wind Technologie GmbH

[10] Haykin S 2009 *Neural networks and learning machines* 3rd ed (Pearson international edition)

[11] Norgaard M, Ravn O and Poulsen N K 2002 *Mathematical and Computer Modelling of Dynamical Systems* **8** 1–20